LOW-POWER ACTIVE INTERFERENCE CANCELLATION FOR OFDM SPECTRUM SCULPTING

Jorge F. Schmidt, Daniel Romero and Roberto López-Valcarce

Department of Signal Theory and Communications
University of Vigo, Spain

ABSTRACT

We present a low-power design for Active Interference Cancellation (AIC) sculpting of the OFDM spectrum, based on sparse design concepts. Optimal AIC designs compute cancellation weights based on contributions from all data subcarriers. Thus, as the number of subcarriers grows, power consumption becomes a concern, and suboptimal solutions that avoid involving all subcarriers are of interest. In this context, we present novel sparse AIC designs based on a zero-norm minimization of the matrix defining the cancellation weights. These designs drastically reduce the number of operations per symbol, and thus the power consumption, while allowing to tune the loss with respect the optimal design. They can be efficiently obtained and significantly outperform usual thresholding or sparsity-inducing ℓ_1-norm minimization approaches.

1. INTRODUCTION

Power consumption of communication technologies has become a concern, both from the service price and from environmental perspectives [1, 2]. In battery-driven mobile devices, as the different signal processing tasks required by current technologies (such as nonlinear front-end impairment compensation, synchronization, spectrum shaping, etc.) become more and more sophisticated, the power spent on these signal conditioning tasks cannot be disregarded. Not only computational capability must be taken into account as a design constraint, but also power consumption. In particular, this paper focuses in low-power designs for OFDM spectrum sculpting.

OFDM is an appealing modulation for cognitive systems whose transmit spectrum must be adjusted to avoid interfering primary users laying within the transmission band. These adjustments can in principle be performed by turning off sets of subcarriers, given the bandwidth partitioning feature of OFDM [3, 4]. However, the high subcarrier sidelobes resulting from the FFT implementation of standard OFDM require the use of more sophisticated spectrum sculpting techniques.

Active interference cancellation (AIC) reserves a small subset of subcarriers to be modulated in order to cancel interference over the protected band, and has received considerable attention recently [5]–[10]. AIC is quite effective and has the advantage of being transparent to the receiver. A power spectral density based AIC scheme (PSD-AIC) recently proposed in [10] employs a fixed linear combination of the data subcarriers to compute the cancellation coefficients, and thus the online computational cost reduces to a matrix-vector product. However, the linear combination matrix involved can be large in practical OFDM implementations, resulting in excessive power consumption. For example, in a system with 1024 subcarriers, with 24 reserved for interference cancellation and 1000 used for data transmission, the optimal AIC design will require 24000 complex multiplications per OFDM symbol. Although it seems intuitive that some (in fact, many) coefficients in this 24×1000 matrix might be discarded in order to reduce the power consumption, obtaining the set of coefficients to retain is not straightforward.

The problem of determining the coefficients to discard given a set of design constraints can be formulated as a zero-norm (cardinality) problem. Zero-norm, or ℓ_0, minimization problems are highly complex combinatorial problems whose solution cannot be obtained in general. Replacing the ℓ_0-norm cost by a surrogate ℓ_1-norm cost, easier to handle analytically, has been a popular and successful approach in compressive sensing applications [11], and has been suggested as well in different problems such as sparse FIR filter design [12] and sparse FIR equalizer design [13]. However, minimization of the ℓ_1-norm does not necessarily imply minimization of the ℓ_0-norm [14]. In [13, 15], heuristic rules were employed to reduce the complexity of the ℓ_0-norm approach for the sparse FIR equalizer/filter design problem. In general, such heuristics must be tailored for the particular problem at hand.

In this context, the main contribution of this paper is to derive sparse designs to reduce power consumption in PSD-AIC. We show that this can be achieved by an approximate ℓ_0-norm minimization, based on the particular structure of the interference matrices involved. An efficient iterative algorithm is provided that meets the design constraints tightly. The performance of the proposed designs is assessed and compared against thresholding and ℓ_1-norm approaches to sparse

design. The proposed schemes result in significantly lower power consumption in all cases.

The paper is organized as follows. The signal model and the optimal non-sparse PSD-AIC solution are presented in Sec. 2. In Sec. 3 the low-power design problem is introduced and the proposed solutions are derived. A performance evaluation is given in Sec. 4, and conclusions are drawn in Sec. 5.

2. PROBLEM STATEMENT

2.1. PSD-AIC Signal Model

Consider a cognitive OFDM transmitter with N subcarriers. A primary system to be protected from interference is known to operate in a frequency band $\mathcal{B}$ spanning N_P contiguous cognitive subcarriers. AIC schemes reserve these N_P subcarriers, plus N_C more to generate a spectrum notch over $\mathcal{B}$, usually under a power budget constraint. This leaves $N_D = N - N_P - N_C$ subcarriers for data transmission. The OFDM signal spectrum is the superposition of all subcarrier spectra, affected by their corresponding modulating coefficients x_k:

$$X(f) = \sum_{k=0}^{N-1} x_k \phi_k(f) = \boldsymbol{x}^T \boldsymbol{\phi}(f), \qquad (1)$$

with $\boldsymbol{\phi}(f) \triangleq [\phi_0(f) \cdots \phi_{N-1}(f)]^T$, $\boldsymbol{x} \triangleq [x_0 \cdots x_{N-1}]^T$, and with

$$\phi_k(f) = M e^{-j\pi \frac{M}{N}\left(\frac{f}{\Delta_f} - k\right)} \operatorname{sinc}_M \left[\frac{1}{N}\left(\frac{f}{\Delta_f} - k\right)\right] \mathcal{G}(f), \qquad (2)$$

the *periodic sinc* spectrum[1] of the k-th subcarrier, times the frequency response $\mathcal{G}(f)$ of the interpolation filter in the D/A converter [16], assumed an ideal brickwall filter retaining only the spectrum replica within the system bandwidth. $M = N + N_{cp}$ is the length of the cyclic-prefix extended symbol, measured in samples, and Δ_f is the subcarrier spacing.

In AIC schemes, the $N \times 1$ vector $\boldsymbol{x}$ in (1) modulating the subcarriers for a given OFDM symbol can be written as $\boldsymbol{x} = \alpha \boldsymbol{S} \boldsymbol{d} + \boldsymbol{T} \boldsymbol{c}$, where $\boldsymbol{d} \in \mathbb{C}^{N_D}$ is the zero-mean data vector, assumed with covariance $E\{\boldsymbol{d}\boldsymbol{d}^H\} = \boldsymbol{I}_{N_D}$, and $\boldsymbol{c} \in \mathbb{C}^{N_P+N_C}$ is the vector of cancellation coefficients. Matrices $\boldsymbol{S} \in \mathbb{C}^{N \times N_D}$ and $\boldsymbol{T} \in \mathbb{C}^{N \times (N_P+N_C)}$ comprise different sets of columns of $\boldsymbol{I}_N$, and map data and cancellation coefficients to the data and reserved subcarrier locations respectively. The scaling factor α ($0 < \alpha \leq 1$) controls how the available transmit power is shared between the data and cancellation subcarriers.

In PSD-AIC [10], cancellation coefficients are linear combinations of the data symbols, i.e., $\boldsymbol{c} = \boldsymbol{\Theta} \boldsymbol{d}$. Hence,

$$\boldsymbol{x} = \boldsymbol{G}(\boldsymbol{\Theta})\boldsymbol{d}, \qquad \text{with} \quad \boldsymbol{G}(\boldsymbol{\Theta}) \triangleq \alpha \boldsymbol{S} + \boldsymbol{T}\boldsymbol{\Theta}, \qquad (3)$$

where $\boldsymbol{\Theta} \in \mathbb{C}^{(N_P+N_C) \times N_D}$ is the design parameter.

---
[1] As in [10], conventional cyclic-prefix OFDM is assumed for simplicity.

2.2. Optimal PSD-AIC

From (1)-(3), and following [16, 10], the signal PSD is obtained in terms of $\boldsymbol{\Theta}$ as

$$P_x(f, \boldsymbol{\Theta}) = E\left\{|X(f)|^2\right\} = \operatorname{Tr}\{\boldsymbol{G}^H(\boldsymbol{\Theta})\boldsymbol{\Phi}(f)\boldsymbol{G}(\boldsymbol{\Theta})\}, \qquad (4)$$

where we have introduced $\boldsymbol{\Phi}(f) \triangleq \boldsymbol{\phi}(f)\boldsymbol{\phi}^H(f)$. Based on (4), the PSD-AIC design problem subject to a power constraint $P_{\max}$ is stated as

$$\min_{\boldsymbol{\Theta}} \int_{\mathcal{B}} P_x(f, \boldsymbol{\Theta})\mathrm{d}f \quad \text{s.t.} \int_{-\infty}^{\infty} P_x(f, \boldsymbol{\Theta})\mathrm{d}f \leq P_{\max}, \quad (5)$$

which is a convex problem. Using the generalized singular value decomposition [17], it is possible to obtain the optimal matrix $\boldsymbol{\Theta}_{\mathrm{opt}}$ efficiently [10].

Fig. 1 illustrates typical PSD-AIC results, for a system with $N = 256$, a target band $\mathcal{B}$ spanning $N_P = 20$ subcarriers, $N_C = 6$ cancellation subcarriers (3 at each side of $\mathcal{B}$), and a 10% power share given to the reserved subcarriers. The PSD $P_0(f) \triangleq P_x(f, \boldsymbol{0})$ obtained by just turning off the reserved subcarriers ($\boldsymbol{c} = \boldsymbol{0}$) is also shown to highlight the sculpting capability of PSD-AIC.
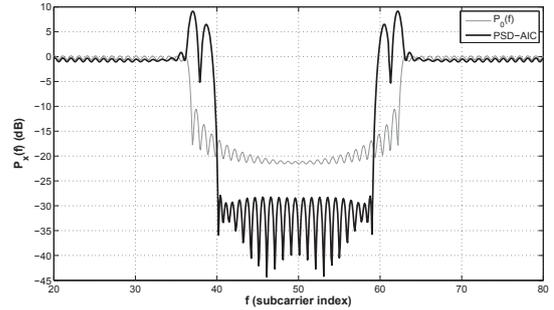
Fig. 1. Typical spectrum sculpting results using PSD-AIC with a target band spanning subcarriers 40 to 59.

Note that $\boldsymbol{\Theta}_{\mathrm{opt}}$ is a non-sparse matrix (i.e. all of its elements are in general nonzero). When the number of system subcarriers is large (and therefore so is N_D) as in current and foreseen OFDM systems, computing $\boldsymbol{\Theta}_{\mathrm{opt}}\boldsymbol{d}$ at each OFDM symbol can be power consuming. Therefore, sparse, and thus low-power suboptimal solutions are of interest.

3. LOW-POWER AIC

The low-power AIC design problem can be stated as finding a weight matrix with as few nonzero elements as possible, while minimizing the power spill over the protected band $\mathcal{B}$ and meeting the power constraint. Let $\boldsymbol{\Psi}$ denote the parameter matrix under some additional sparsity constraint. As we know the optimal matrix solving (5) is non-sparse, one has

$$\min_{\boldsymbol{\Psi}} \int_{\mathcal{B}} P_x(f, \boldsymbol{\Psi})\mathrm{d}f \geq \int_{\mathcal{B}} P_x(f, \boldsymbol{\Theta}_{\mathrm{opt}})\mathrm{d}f \triangleq P_{\mathcal{B}}, \quad (6)$$

when both optimizations are subject to the same power constraint. Therefore, we introduce a design parameter $\gamma > 1$ quantifying the performance loss with respect to Θ_{opt}. Also introduce the $N \times N$ Hermitian matrices

$$\Phi_{\mathcal{B}} \triangleq \int_{\mathcal{B}} \Phi(f)\mathrm{d}f, \quad \Phi_{\mathcal{T}} \triangleq \int_{-\infty}^{\infty} \Phi(f)\mathrm{d}f, \qquad (7)$$

so that, with $\psi \triangleq \mathrm{vec}(\Psi)$, the low-power design is stated as

$$\min_{\psi} \|\psi\|_0 \quad \text{s.t.} \begin{cases} \mathrm{Tr}\{G^H(\Psi)\Phi_{\mathcal{T}}G(\Psi)\} \leq P_{\max}, \\ \mathrm{Tr}\{G^H(\Psi)\Phi_{\mathcal{B}}G(\Psi)\} \leq \gamma P_{\mathcal{B}}, \end{cases} \qquad (8)$$

where $\|\cdot\|_0$ is the ℓ_0-norm (number of nonzero entries).

Given the dimensions of the matrices involved, the complexity of the combinatorial problem (8) precludes a direct solution. Alternatively, we propose a two-step iterative algorithm[2] that searches for a near-optimal sparse solution Ψ_*, considering the constraints separately. The algorithm is initialized with the non-sparse solution Θ_{opt}, and iterates between the two steps described next, until no further weights can be discarded; this is summarized in Algorithm 1.

Algorithm 1 Low-power AIC design

Initialization: $n = 0$, $\Psi_0 = \Theta_{\text{opt}}$
  repeat
    • $n \leftarrow n + 1$
    • Obtain $\tilde{\Psi}_n$ by zeroing elements from Ψ_{n-1} according to **Step 1**.
    • Obtain Ψ_n by reoptimizing the nonzero elements of $\tilde{\Psi}_n$ according to **Step 2**.
  until $\|\psi_n\|_0 = \|\psi_{n-1}\|_0$
  Output: $\Psi_* = \Psi_n$

3.1. Step 1: Weight elimination

Consider the zero-norm minimization in (8) taking into account only the performance loss constraint. Let us define

$$Q \triangleq T^T \Phi_{\mathcal{B}} T, \quad q_i^H \triangleq 2\alpha s_i^T \Phi_{\mathcal{B}} T, \qquad (9)$$

with s_i ($i = 1, \ldots, N_D$) the columns of S. Inserting the expresion for $G(\Psi)$ from (3) in (4) and rearranging using (9), the weight elimination subproblem can be expressed as

$$\min_{\psi} \|\psi\|_0 \quad \text{s.t.} \ P_{0\mathcal{B}} + \psi^H \mathcal{Q}\psi + \mathrm{Re}\{\tilde{q}^H \psi\} \leq \gamma P_{\mathcal{B}}, \quad (10)$$

where $P_{0\mathcal{B}} \triangleq \alpha^2 \mathrm{Tr}\{S^T \Phi_{\mathcal{B}} S\}$ and

$$\mathcal{Q} \triangleq I_{N_D} \otimes Q, \qquad \tilde{q} \triangleq [q_1^T \ q_2^T \ \cdots \ q_{N_D}^T]^T. \quad (11)$$

A problem analogous to (10) has been considered in [15] from the perspective of sparse filter design, where a procedure to obtain the optimal solution for the structure of $\mathcal{Q}$ in

(10) was derived. However, such approach is too computationally demanding due to the large size ($N_P + N_C$) of the block-diagonal elements Q. In [15] a greedy approach is also proposed, which is shown to yield the optimal solution if $\mathcal{Q}$ in (10) is diagonal. Although this is not the case in general, the strong diagonal structure of the block diagonal element Q makes such greedy approach a good candidate for obtaining a near-optimal solution. Specifically, note that Q is a submatrix of $\Phi_{\mathcal{B}}$ in (7), and thus its elements are given by

$$\Phi_{\mathcal{B}}^{(i,j)} = \int_{\mathcal{B}} \phi_i(f)\phi_j^H(f)\mathrm{d}f, \qquad (12)$$

for i, j within the index set of reserved subcarriers. Since the functions $\phi_i(f)$ correspond to the spectrum of OFDM subcarriers, each row of Q is maximum for $i = j$ and its magnitude rapidly drops as $|i - j|$ increases[3]. Further, this near diagonal behavior is stronger for the N_P subcarriers within band $\mathcal{B}$ (usually most of the reserved subcarriers), since their main lobe is included in the integral. Thus, we replace the constraint in (10) by

$$P_{0\mathcal{B}} + \sum_{i=1}^{(N_P+N_C)N_D} \underbrace{\left[\mathcal{Q}(i,i)|\psi(i)|^2 + \mathrm{Re}\{\tilde{q}^*(i)\psi(i)\}\right]}_{\triangleq \rho(i)} \leq \gamma P_{\mathcal{B}}. \qquad (13)$$

At this point, we take $\psi = \mathrm{vec}(\Psi_{n-1})$ from the previous iteration, and proceed to discard the elements of ψ with the smallest associated contribution $\rho(i)$ until right before the constraint in (10) is no longer met. The resulting matrix and the corresponding set of zero coefficients are denoted by $\tilde{\Psi}_n$ and $\mathcal{M}_n$ respectively. Despite the approximation introduced in (13), simulation results in Sec. 4 will show that the number of nonzero weights is effectively reduced.

3.2. Step 2: Weight update

The procedure in **Step 1** allows to reduce the number of active (nonzero) weights, but now it becomes necessary to reoptimize these active weights and also to ensure that the original power constraint in (8) is satisfied. This results in the following problem:

$$\min_{\Psi} \int_{\mathcal{B}} P_x(f, \Psi)\mathrm{d}f \quad \text{s.t.} \begin{cases} \int_{-\infty}^{\infty} P_x(f, \Psi)\mathrm{d}f \leq P_{\max}, \\ \Psi(i,j) = 0 \quad \text{for } (i,j) \in \mathcal{M}_n. \end{cases} \qquad (14)$$

Note that Problem (14) has a convex objective and convex constraints. In fact, the constraints $\Psi(i,j) = 0$ for $(i,j) \in \mathcal{M}_n$ can be removed by expressing $P_x(f, \Psi)$ in terms of the nonzero elements of Ψ only, and optimizing with respect to these variables following the same procedure as in [10] for the original problem (5).

---

[2]Note that the proposed algorithms are applied at the design stage, and hence they do not affect implementation (online) cost.

[3]This is a general property of multicarrier modulations, and not just of conventional OFDM as considered here.
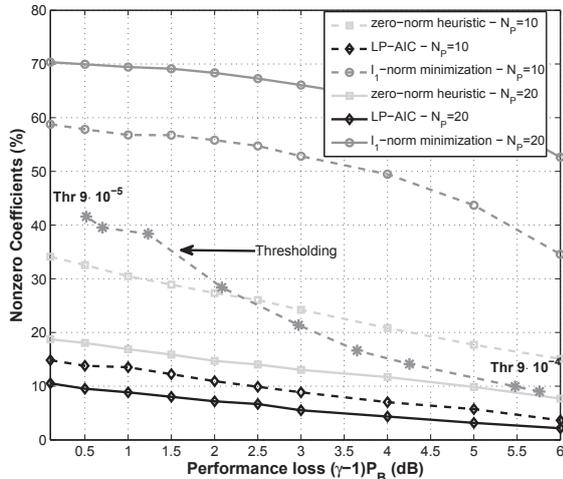
Fig. 2. Sparsity vs. performance loss using different designs.

4. PERFORMANCE EVALUATION

The performance of the proposed low-power design, termed LP-AIC in what follows, is evaluated next. The sparsity obtained in the matrix of linear combination weights is assessed under different settings and compared against two alternative designs. The first one is a simplified scheme by which the ℓ_0-norm heuristic of Sec. 3.1 is applied to the optimal non-sparse matrix $\mathbf{\Theta}_{opt}$ to discard some of its coefficients, without any further refinement; we term this scheme "ℓ_0-norm heuristic." The second design replaces the ℓ_0-norm in (8) with the surrogate ℓ_1-norm[4], and is termed "ℓ_1-norm minimization."

We consider an OFDM system with $N = 256$ subcarriers and a 5% (12 samples) cyclic prefix. The protected band $\mathcal{B}$ spans subcarriers $40 - 49$ or $40 - 59$, to obtain target bandwidths of $N_P = 10$ or 20 subcarriers respectively. $N_C = 6$ additional subcarriers are reserved for protection improvement, 3 at each side of $\mathcal{B}$ as in Fig. 1. In all cases the power share given to the reserved subcarriers is set to 10%. The parameter γ in (8) is adjusted such that different loss targets from the non-sparse optimal solution of (5) are obtained.

Fig. 2 shows the degree of sparsity in the weight matrix obtained by the three designs considered for $N_P \in \{10, 20\}$, as a function of the target loss. The proposed LP-AIC design significantly outperforms the other two methods in all cases, yielding the smallest amount of nonzero coefficients even for low degradation targets. Specifically, in the most stringent case ($N_P = 10$ and 0.1 dB loss), the percentage of nonzero coefficients is just 14.8%. At the other extreme ($N_P = 20$ and allowing a 6 dB loss) this percentage drops to a mere 2.2%.

For $N_P = 10$, Fig. 2 also shows results obtained with a

straightforward thresholding approach[5]. Clearly, this method fails to provide good results for small to moderate losses.

It is observed that the ℓ_1-norm design performs considerably worse than the schemes based on the ℓ_0-norm. Note also that, as the band to be protected becomes wider, the percentage of nonzero coefficients decreases for the ℓ_0-norm based designs, whereas on the contrary it increases for the ℓ_1-norm minimization. The sparsity patterns obtained for each scheme give a better insight into this behavior.
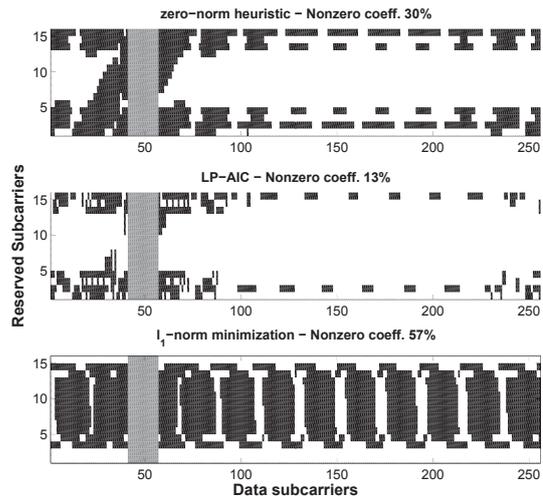
Fig. 3. Sparsity patterns ($N_P = 10$ and 1 dB loss).

Fig. 3 shows the resulting sparsity patterns of the weight matrices for $N_P = 10$ and 1 dB performance loss. These patterns are a graphical representation of the matrix $\mathbf{\Theta}$ in (3). There are $N_P + N_C = 16$ rows in each plot corresponding to the reserved subcarriers, and $N = N_D + 16 = 256$ columns corresponding to the system subcarriers. The 16 gray columns are not part of $\mathbf{\Theta}$, but are inserted to emphasize where the target band is located. Nonzero elements are plotted in black. Note that, in the first two subplots corresponding to the ℓ_0-norm based designs, most of the zero elements correspond to the reserved subcarriers aligned with the protected band. This happens because those subcarriers cannot be allocated much power (see example in Fig. 1) and are thus good candidates for being discarded using the heuristic in Sec. 3.1. The opposite trend is observed for the ℓ_1-norm minimization design (third subplot): since those weights have a small contribution to the overall ℓ_1-norm, the minimizer of this objective function tends to discard more high-power cancellation subcarriers outside the protected band. Therefore, ℓ_0-norm approaches are found to better exploit the particular structure of the AIC problem than the ℓ_1-norm minimization

---

[4]This change makes the problem in (8) convex, such that it can be solved for the optimal solution using adequate convex solvers. These optimal solutions are the ones used for comparison.

[5]Specifically, the ℓ_1-norm of vec($\mathbf{\Theta}_{opt}$) is normalized to 1, and all normalized elements below a defined *threshold* are dropped. Then, the remaining elements are recomputed following Sec. 3.2.
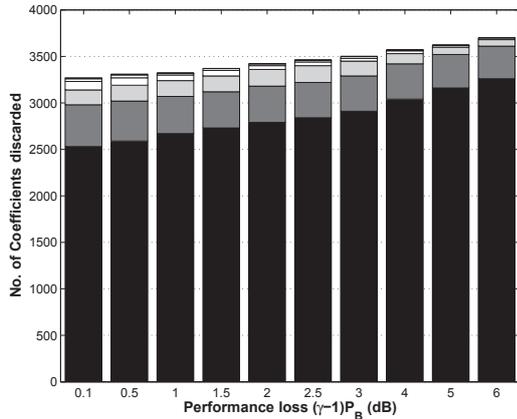
Fig. 4. Sparsity improvement per iteration for LP-AIC and different loss targets. Results are shown for $N_P = 10$.

scheme. This phenomenon has also been reported in different contexts (see e.g. [18, 15]) and is due to the fact that the conditions for ℓ_1-norm relaxation to provide the ℓ_0-norm solution are not satisfied in the problem at hand [14].

Our last experiment focuses on the advantage of LP-AIC with respect to the ℓ_0-norm heuristic. The main difference between these schemes is that LP-AIC recomputes the optimal matrix after each ℓ_0-norm reduction step, allowing further iterations to obtain a sparser solution meeting the constraints more tightly. Fig. 4 shows the amount of coefficients discarded in each iteration of LP-AIC for different performance targets with $N_P = 10$. Observe that most coefficients are discarded in the first iteration (82.4% for a 6 dB target loss), corresponding to the ℓ_0-norm heuristic scheme, and 11.4, 4.2, 1.4 and 0.5% in subsequent iterations. Thus, a near optimal solution can be found with as few as two or three iterations.

5. CONCLUSIONS

We have proposed a novel low-power AIC design based on an ℓ_0-norm minimization algorithm that iteratively removes elements from the non-sparse optimal PSD-AIC matrix of linear combination coefficients and readjusts surviving weights. The proposed design drastically reduces the power consumption of AIC as only a small fraction of nonzero weigths is kept. The proposed design significantly outperforms the standard thresholding or ℓ_1-norm approaches, which are not able to exploit the particular structure of the AIC problem.

6. REFERENCES

[1] V. Mancuso and S. Alouf, "Reducing costs and pollution in cellular networks," *IEEE Commun. Mag.*, vol. 49, no. 8, pp. 63–71, 2011.

[2] K. Hinton, J. Baliga, M. Feng, R. Ayre, and R. Tucker, "Power consumption and energy efficiency in the internet," *IEEE Network*, vol. 25, no. 2, pp. 6–12, 2011.

[3] T. A. Weiss and F. K. Jondral, "Spectrum pooling: an innovative strategy for the enhancement of spectrum efficiency," *IEEE Commun. Mag.*, vol. 42, no. 3, pp. S8–14, Mar. 2004.

[4] H. Arslan, H. A. Mahmoud, and T. Yucek, "OFDM for cognitive radio: merits and challenges," in *Cognitive Radio, Software Defined Radio, and Adaptive Wireless Systems*, H. Arslan, Ed. Dordrecht, The Netherlands: Springer, 2007.

[5] H. Yamaguchi, "Active interference cancellation technique for MB-OFDM cognitive radio," in *34th Eur. Microwave Conf.*, vol. 2, Oct. 2004, pp. 1105 –1108.

[6] E. H. M. Alian, H. E. Saffar, and P. Mitran, "Cross-band interference reduction trade-offs in SISO and MISO OFDM-based cognitive radios," *IEEE Trans. Wireless Commun.*, vol. 11, no. 7, pp. 2436–45, Jul. 2012.

[7] E. H. M. Alian and P. Mitran, "Improved active interference cancellation for sidelobe suppression in cognitive OFDM systems," in *IEEE Global Commun. Conf. (GLOBECOM)*, Dec. 2012, pp. 1460–65.

[8] J. F. Schmidt and R. López-Valcarce, "Low complexity primary user protection for cognitive OFDM," in *Eur. Signal Process. Conf. (EUSIPCO)*, Sep. 2013.

[9] ——, "OFDM spectrum sculpting with active interference cancellation: keeping spectral spurs at bay," in *IEEE Int. Conf. Acoust., Speech, Signal Process.*, May 2014.

[10] J. F. Schmidt, S. Costas-Sanz, and R. López-Valcarce, "Choose your subcarriers wisely: Active interference cancellation for cognitive OFDM," *IEEE J. Emerg. Sel. Topics Circuits Syst.*, vol. 3, no. 4, Dec. 2013.

[11] E. J. Candès and M. Wakin, "An introduction to compressive sampling," *IEEE Signal Process. Mag.*, vol. 25, no. 2, pp. 21–30, 2008.

[12] T. Baran, D. Wei, and A. V. Oppenheim, "Linear programming algorithms for sparse filter design," *IEEE Trans. Signal Process.*, vol. 58, no. 3, pp. 1605–1617, 2010.

[13] A. Gomaa and N. Al-Dhahir, "A new design framework for sparse FIR MIMO equalizers," *IEEE Trans. Commun.*, vol. 59, no. 8, pp. 2132–2140, 2011.

[14] E. J. Candès, J. Romberg, and T. Tao, "Robust uncertainty principles: exact signal reconstruction from highly incomplete frequency information," *IEEE Trans. Inf. Theory*, vol. 52, no. 2, pp. 489–509, Feb. 2006.

[15] D. Wei, C. K. Sestok, and A. V. Oppenheim, "Sparse filter design under a quadratic constraint: Low-complexity algorithms," *IEEE Trans. Signal Process.*, vol. 61, no. 4, pp. 857–870, 2013.

[16] T. van Waterschoot, V. Le Nir, J. Duplicy, and M. Moonen, "Analytical expressions for the power spectral density of CP-OFDM and ZP-OFDM signals," *IEEE Signal Process. Lett.*, vol. 17, no. 4, pp. 371 –374, Apr. 2010.

[17] G. H. Golub and C. F. van Van Loan, *Matrix Computations*, 3rd ed. The Johns Hopkins University Press, Oct. 1996.

[18] L. Mancera and J. Portilla, "L0-norm-based sparse representation through alternate projections," in *IEEE Int. Conf. Image Process.*, 2006, pp. 2089–2092.